A SEARCH FOR SHORT TIMESCALE MICROVARIABILITY IN ACTIVE GALACTIC NUCLEI IN THE ULTRAVIOLET

Joseph F. Dolan
Laboratory for Astronomy and Solar Physics
NASA Goddard Space Flight Center
Greenbelt, MD 20771-6810
Joseph.F.Dolan@nasa.gov

L. Lee Clark
Department of Astronomy
San Diego State University
San Diego, CA 92182-1221
clark@sciences.sdsu.edu

Running Head: MICROVARIABILITY IN AGNS

ABSTRACT

We observed four AGNs (the type-1 Seyfert systems 3C249.1, NGC 6814 and Mrk 205, and the BL Lac object 3C371) using the High Speed Photometer on the Hubble Space Telescope to search for short timescale microvariability in the UV. Continuous observations of ~3000 s duration were obtained for each system on several consecutive HST orbits using a 1 s sample time in a 1400 - 3000 Å bandpass. No photometric variability > 0.3% (0.003 mag) was detected in any AGN on timescales shorter than 1500 s. The distribution of photon arrival times observed from each source was consistent with Poisson statistics. Because of HST optical problems, the limit on photometric variability at longer timescales is less precise. These results restrict models of supermassive black holes as the central engine of an AGN and the diskoseismology oscillations of any accretion disk around such a black hole.

Key words: Galaxies: Active - Galaxies: Individual: NGC 6814; Mrk 205; 3C249.1; 3C371 - Ultraviolet: Galaxies

1. INTRODUCTION

Photometric variability appears to be an intrinsic property of active galactic nuclei (AGNs). Seyfert-type AGNs exhibit fluctuations in the visible of several per cent on a timescale of days (Ulrich et al. 1997 and references therein). Short timescale variability ($t < 10^{3-4}$ s) is a distinguishing characteristic of Seyfert-1 type AGNs in the X-ray region, and the variability is sometimes quasi-periodic (Liszka et al. 2000). Quasi-stellar objects (QSOs) can exhibit large amplitude variability at all wavelengths on a timescale of days or less (Wagner & Witzel 1995).

The maximum characteristic dimension, D, associated with the central power source of AGNs is limited by the shortest timescale of variability, T, present in its radiative emission. Nominally, $D = cT/(1 + z)$. For black holes (BHs) in the mass range 10^{6-9} $M_\odot$, the current consensus candidate for the central engine of AGNs (Kormendy & Richstone 1995), the innermost stable orbit around a Schwarzschild (non-rotating, non-charged) BH has period

$$p = 600\ M_6\ \text{s}, \quad [1]$$

where M_6 is the mass of the BH in units of 10^6 $M_\odot$ (Sunyaev 1973). The innermost stable orbits around a rotating (Kerr) BH have periods less than this; for a maximally rotating Kerr BH, $p = 60\ M_6$ s (Novikov & Thorne 1973). Any periodic variability from an AGN having a timescale in this range would necessarily arise in the inner region of the accretion disk around the central BH. The mass of the BH could be inferred from the period of the variability.

General relativity requires the existence of a spectrum of adiabatic oscillations in a thin, Keplerian disk around a BH. The oscillations are trapped near the inner edge of a disk which is terminated at its innermost marginally stable orbit (Nowak & Wagoner 1991; 1992). For g-modes in diskoseismology, analogous to the acoustic waves of helioseismology, the highest frequency modes predominantly involve vertical motion in the inner disk. The periods expected are on the order of $10^3 M_6$ s (Nowak & Wagoner 1993; Perez et al 1997; Nowak et al. 1997). The luminosity modulation of the inner disk region is calculated to be large in the UV - a factor of 10 or more. Because the inner disk is highly luminous, these oscillations might cause periodic photometric variability on the order of 1% in AGNs in the UV.

For both of these reasons, we decided to search for short timescale ($t < 10^{3-4}$ s) microvariability ($\Delta I/I < 0.01$) in AGNs in the ultraviolet region of the spectrum. We report here the results for four AGN systems: 3C249.1, NGC 6814, and Mkn 205, all type-1 Seyferts with a QSO at their nucleus; and the BL Lac object 3C371.

2. OBSERVATIONS

The journal of our observations is given in Table 1. All observations were taken continuously with a 1 s sample time using the F140LP filter on the UV2 detector of the High Speed Photometer (HSP). The full width bandpass at 1/e of maximum throughput of the F140LP filter for a flat incident spectrum extends between 1400 and 3000 Å (Bless et al. 1992). A 10.0" diameter aperture was used for all observations except those of NGC 6814, for which a 1.0" aperture was used. The brightest point of the nucleus was centered in the aperture in each case. The fluxes given in Table 1 were derived using the conversion factor 1 detected count s^{-1} = 3.73 ± 0.07 μJy in the F140LP bandpass; their stated uncertainty includes both the systematic uncertainty in the conversion factor, which dominates, and the statistical uncertainty in the observed count rate.

The observations were taken using gyroscopic control of the pointing of the Hubble Space Telescope (HST). Slow drifts in the pointing led to significant linear decreases in counting rate with time in the last three observations of 3CR371. As a result, no value of the flux from 3CR371 was obtained from these three observations. No other data sets were affected by this type of gyro drift, although each of the Mkn 205 observations exhibited a single short loss of data extending over a time ranging from 3 to 27 s caused by temporary loss of lock by the gyros. The fluxes given in Table 1 for Mkn 205 were measured outside of these intervals.

Orbit-to-orbit variations in the counting rate observed by the HSP from a constant source are caused by the HST breathing effect (Bless et al. 1999) - changes in the position of the secondary mirror resulting from variable heating of the spacecraft around its orbit. If a significant fraction of the image's spherically aberrated point spread function is vignetted by the observing aperture, the resulting motion of the image on the detector results in a sinusoidal variation in the detected flux at the period of the HST orbit, 94.06 min (Taylor et al. 1993). This effect can be seen as similarly shaped long-timescale variability in observations of NGC 6814 taken on successive orbits through the 1.0" aperture.

We successfully minimized the breathing effect for sources other than NGC 6814 by observing through the 10" aperture, the diameter of which was significantly larger than the > 2" diameter of a point source's 90% encircled energy region (Bless et al. 1999). Even so, variability at the orbital period can be detected in all our data sets. We are convinced from experience with many observations of constant sources that breathing is the cause of any variability with the orbital period we see in these observations. The variability caused by breathing can be easily removed from a single continuous observation (cf. Taylor et al. 1993), but it seriously compromises our ability to relate measured fluxes from two discontinuous observations taken during different HST orbits. We accordingly view with extreme caution any variability detected with a timescale longer than the duration of a single continuous observation.

3. DATA ANALYSIS

The type of statistics governing the distribution of arrival times of photons from each source was investigated under the assumptions of the χ^2 test. The variability of each data set on a 1 s time scale is consistent at the 90% level of confidence with a Poisson distribution of photon arrival times from a constant intensity source with variance equal to its mean.

Periodic and quasi-periodic variability were searched for at timescales > 2 s using power spectrum analysis and auto- and cross-correlation analysis. The last three observations of 3CR371 were analyzed for variability by first subtracting the linear slope which best represented the time-variable mean of the data, converting them to stationary data sets. The short stretch of missing data in each of the Mkn 205 data sets was replaced by random Gaussian data having the same mean and variance as the rest of the data set.

The power spectrum function (PSF) was calculated for each individual data set. This analysis method is most sensitive to sinusoidally shaped variability. The significance of the results was evaluated using Fisher's test of significance in PSFs (Fisher 1929; Shimshoni 1971). A mean PSF for all observations of the same source was derived by adding the individual PSFs together and dividing by n, the number of individual data sets. Assuming that a constant intensity periodic signal is present in all data sets in a background of random noise, the level of significance of Fisher's g statistic is decreased by the factor $1/\sqrt{n}$ below its value for a single data set. Upper limits to any non-detected signal were estimated by adding a sinusoid of known period to the data and determining the amplitude at which its PSF frequency reached the 0.01 level of significance.

Auto-correlation functions (ACFs) were calculated for each individual data set. The ACF is most sensitive to delta-function shaped variability. The "characteristic timescale" of variability, defined as the time it takes the ACF to drop to 1/e from its value of unity at zero lag (Mittaz & Branduardi-Raymont 1989), is < 1 s for every data set, as required for a distribution in photon arrival times consistent with Poisson statistics. The expectation value at each lag time of the ACF of a random data set with no periodic signal in it is -1/N, where N is the number of samples in the data set, and the standard deviation is $1/\sqrt{N}$ (Chatfield 1996). We considered a peak in the ACF significant at the 3σ (0.0027) level of significance. Upper limits to non-detected signals were estimated by adding a Kronecker delta-function to the data at a known period and determining the amplitude at which the ACF at that lag time reached the 3σ level of significance.

Searches for variability on timescales longer than one data set were carried out by calculating the cross-correlation function of one data set with a later one. We also formed a total data set by concatenating the individual data sets with embedded strings of zeroes at the running epoch of each observation. ACFs were calculated for the total data sets.

4. RESULTS

4.1. 3C249.1

The lobe-dominated radio source 3C249.1 is a type-1 Seyfert galaxy (Stockton & MacKenty 1983) with a quasi-stellar object at its nucleus ($z = 0.313$, $B = 15.70$, $B - V = -0.02$, $l = 130.39^{\circ}$, $b = +38.55^{\circ}$) (Hewitt & Burbidge 1987). It is also an X-ray source.

Although 3C249.1 is a stable flux calibration source in the radio region of the spectrum (Astron. Almanac 1997), the QSO has been observed to vary by 0.08 mag over 2 hours in the r band (Jang & Miller 1997) and by 0.25 mag over a day in the visible (Penston & Cook 1970). Longer timescale variability in the visible is reported by Netzer et al. (1996) and Lloyd (1984).

The first data set obtained from 3C249.1 is shown in Fig. 1, and is typical of all six data sets. The PSF of this data set is shown in Fig. 2. The Fisher g statistic equals or exceeds 0.00875 (0.00757) in some frequency bin for 1% (5%) of all random data sets having the same number of data points as this data set. No significant periodic signal was visible in the PSF of any observation of 3C249.1.

The ACF of the same data set is shown in Fig. 3. The 3σ level of significance for 2688 data points lies at 0.0579; the largest positive excursion of the ACF, at 385 s lag time, reaches 0.0569. (Note the larger negative excursion, -0.0625, at 1255 s lag time. Excursions at or above the 3σ

level occur on average 3.6 times in 1344 lag time calculations for a random data set with no signal in it.) Large positive excursions of the ACF were examined further by binning the original data set modulo the period of the excursion. No coherent light curves were revealed, even after binning several adjacent phases to increase the statistical significance of each resulting data point. No significant signal was visible in the ACF of any observation of 3C249.1.

Upper limits on the pulsed fraction of any periodic signal below our limit of detectability were calculated by the methods given in Sec. 3 above. We define the pulsed fraction, PF, as the fraction of the total flux in the periodic component, or PF = S/T, where S is the time-averaged flux in the signal, and T is the time-averaged flux from the source. The 3σ upper limit on any periodic signal from 3C249.1 in the 1400 - 3000 Å bandpass at the epoch of our observations is PF < 0.3% (0.003 mag) for all timescales between 2 and 1344 s.

4.2. NGC 6814

The type-1 Seyfert galaxy NGC 6814 is morphologically an Sbc galaxy (B = 12) at z = 0.0052, $l = 29.35^{\circ}$, $b = -16.01^{\circ}$. It is also an X-ray source (Cooke et al. 1973). Although NGC6814 was reported by several observers to have a 12,117 s periodic signal in its X-ray flux (cf. Mushotzky et al. 1993), this variability was later ascribed to a cataclysmic variable 37' away in the same field (Madejski et al. 1993;

Staubert et al. 1994). NGC 6814 is a highly variable X-ray source on timescales longer than a few hundred seconds (Konig et al. 1997), although the variability is not periodic. In the visible, NGC 6814 varies by 0.15 mag over a timescale of days (Webb & Malkan 2000; Winkler et al. 1992).

The data obtained from our three observations are shown in Fig. 4, with the being gaps caused by Earth occultations. The slope visible at the beginning of the first and third data sets is typical of the effect caused by breathing. This variation with orbital period was the only significant signal in the PSF of the data, appearing in the frequency bin at 1 cycle per 2400 s, and being significant only in the average PSF of the three data sets.

ACFs and CCFs were also calculated for individual data sets. Although the ACF of each data set drops below a value of 1/e at the first lag time of 1 s, consistent with our finding of Poisson statistics from the source, there is a significant slope to the ACF which is caused by breathing. The breathing effect is most visible in our observations of NGC 6814 because these were the only ones obtained using a 1.0" aperture (to better isolate the nuclear region of the galaxy). No significant signal was otherwise observed in any ACF.

The 3σ upper limit on any periodic signal from NGC 6814 in the 1400 - 3000 Å bandpass at the epoch of our observations is PF < 0.9% (0.009 mag) for timescales between 2 and 1200 s.

4.3. Mrk 205

The Markaryan galaxy Mrk 205 is a type-1 Seyfert with the QSO B1219+7535 at its nucleus (z = 0.0708, B = 14.50, l = 125.45°, b = $+41.67^\circ$). There have been discussions in the literature of a possible physical connection between Mrk 205 and NGC 4319, a spiral galaxy at z = 0.005 (Sulentic & Arp 1987), but the evidence remains inconclusive (Cecil & Stockton 1985). Mrk 205 varies photometrically in the visible by amounts up to 50% over several years (Kuhn et al. 1991).

No statistically significant variability was detected in any PSF or ACF of the Mrk 205 data sets. The 3σ upper limit on any periodic signal from Mrk 205 in the 1400 - 3000 Å bandpass at the epoch of our observations is PF < 0.3% (0.003 mag) for timescales between 2 and 1344 s.

4.4. 3C371

The BL Lac object 3C371 (z = 0.051, B = 14.4, l = 100.13°, b = $+29.17^\circ$) exhibits a composite spectrum containing the stellar absorption line spectrum of an E galaxy, emission lines similar to those found in some giant E galaxies, and a strong nonthermal continuum like many BL Lac objects (Miller 1975). A radio/optical jet is associated with the source (Nilsson 1997). The QSO and its jet are both X-ray sources (Pesce et al. 2001).

3C371 varies in the visible by 1.5 mag over a timescale of years and has exhibited variations up to 0.2 mag over a timescale of hours (Carini et al. 1998) to days (Oke 1967). Carini et al. also report 0.06 mag brightness excursions lasting 60 minutes in the V band.

The first 200 s of data we obtained from 3C371 during the first observation listed in Table 1 (Fig. 5) shows the typical variations present in individual counting rate samples. The distribution of intervals between photon arrival times is consistent with Poisson statistics. No statistically significant variability was detected in any PSF or ACF of the 3C371 data sets. The 3σ upper limit on any periodic (or quasi-periodic) signal in the UV from 3C371 for timescales between 2 and 1620 s is PF < 0.4% (0.004 mag).

5. DISCUSSION

The results presented here are similar to those reported by Welsh et al. (1998, hereafter W98), who found no variability in the type-1 Seyfert NGC 7469 on timescales of minutes to hours in the UV. These are the only other UV observations of short timescale microvariability in AGN that we are aware of in the literature. The bandpass used by W98 was nominally 1500 - 3400 Å, but was contaminated by "a considerable amount" of visible light and light from emission lines outside this bandpass. W98 estimate that a periodic signal existing during their 11.5 hour observing window with PF > 0.2% (1σ UL) would have been detected in their data.

We rebinned our first observation of 3C371 into 45 s long samples (Fig. 6) after first correcting for the breathing effect so that it could be compared directly with the variation in counting rates reported by W98 for NGC 7469 (Figs. 4 and 5 in W98). The data shown by W98 appears somewhat noisier than our continuous data. This is caused by W98's data containing only 10.64 s of exposure time on 44.5 s centers and their incomplete removal of a systematic effect (geomagnetically induced image motion) affecting the photometric stability of the Faint Object Spectrograph with which the data was obtained.

Falomo et al. (2002) estimate the mass of the BH in the nucleus of several BL Lac objects using the virial theorem and the stellar velocity dispersion in the host E galaxy.

They derive a mass of 800 M_6 for the BH mass in 3C371. If the BH mass in 3C371 were this large, the characteristic timescale associated with the innermost stable orbit of a surrounding accretion disk would be 9,000 - 90,000 s, depending on the angular momentum of the BH. Our observations would not have detected any periodic variations with this long a timescale.

The lack of detection of any periodic (or quasi-periodic) variability in AGNs by both W98 and ourselves may indicate that such variability does not exit (or is not common), or it may indicate that the mass of any BH in the nucleus of AGNs is more massive than 3 - 30 M_6, the mass limit set by Eq. [1] and our longest detectable periodicity. We note that the minimum mass derived by Falomo et al. (2002) for any of the seven BL Lac objects they studied is 150 M_6.

The upper limit on microvariability in AGNs we determined, PF < 0.3%, is near the level of variability expected from disk oscillations predicted by the theory of diskoseismology. This null result is also consistent with the theory if BH masses are >> 10^6 $M_\odot$ in AGNs, because then the characteristic period of the oscillations would be longer than our longest detectable periodicity.

These observations were made using the Hubble Space Telescope, which is operated by AURA, Inc. at the Space Telescope Science Institute under NASA contract NAS5-26555. JD acknowledges the hospitality of the Department of

Astronomy at San Diego State University, where much of this work was carried out.

TABLE 1

1400 - 3000 Å Bandpass Observations

Source	Starting Time (JD 244 0000 +)	Length (s)	Flux (mJy)
3C249.1	8912.215833	2688	1.78 ± 0.03
	8912.282731	"	1.76 0.03
	8912.349641	"	1.77 0.03
	8912.416551	"	1.77 0.03
	8912.483449	"	1.78 0.03
	8912.550359	"	1.78 0.03
NGC 6814[a]	8921.737002	2400	0.295 ± 0.006
	8921.803704	"	0.295 0.006
	8921.870683	"	0.292 0.006
Mkn 205	8981.185243	2688	2.86 ± 0.05
	8981.252176	"	2.83 0.05
	8981.319086	"	2.82 0.05
	8981.385984	"	2.81 0.05
	8981.452917	"	2.81 0.05
	8981.519838	"	2.81 0.05
3CR371	9054.153171	3240	1.47 ± 0.03
	9054.217211	"	1.45 0.03
	9054.283900	"	b
	9054.350613	"	b
	9054.417338	"	b

a 1.0" diameter aperture. All other observations used a 10.0" aperture.

b See text.

REFERENCES

Astronomical Almanac 1997 (Washington: U.S. Govt. Printing Office)

Bless, R. C., et al. 1999, P.A.S.P., 111, 364

Carini, M. T., Noble, J. C., & Miller, H. R. 1998, AJ, 116, 2667

Cecil, G., & Stockton, A. 1985, ApJ, 288, 201

Chatfield, C. 1996, The Analysis of Time Series (London: Chapman & Hall)

Cooke, B. A., et al. 1978, MNRAS, 182, 489

Falomo, R., Kotilainen, J. K., & Treves, A. 2002, ApJ, 569, L35

Fisher, R. A. 1929, Proc. Roy. Soc. A, 125, 54

Hewitt, A., & Burbidge, G. 1987, ApJS, 63, 1

Jang, M., & Miller, H. R. 1997, AJ, 114, 565

Konig, M., Friedrich, S., Staubert, R., & Timmer, J. 1997, A&A, 322, 747

Kormendy, J., & Richstone, D. 1995, ARA&A. 33, 581

Kuhn, O., Siemiginowska, A., Elvis, M. Wilkes, B. J., & McDowell, J. 1991, BAAS, 23, 926

Liszka, L., Pacholczyk, A. G., & Stoeger, W. R. 2000, ApJ, 540, 122

LLoyd, C. 1984, MNRAS, 209, 697

Madejski, G. M., et al. 1993, Nature, 365, 626

Miller, J. S. 1975, ApJ, 200, L55

Mittaz, J. P. D., & Branduardi-Raymont, G. 1989, MNRAS, 238, 1029

Mushotzky, R. F., Done, C., & Pounds, K. A. 1993, ARA&A, 31, 717

Netzer H., et al. 1996, MNRAS, 279, 429

Nilsson, K., Heidt, J. Purismo, T., Sillanpaa, A., Takalo, L. O., & Jager, K. 1997, ApJ, 484, L107

Novikov, I. D., & Thorne, K. S. 1973, in Black Holes, ed. C. DeWitt & B. S. DeWitt (New York: Gordon & Breach), 343

Nowak, M. A., & Wagoner, R. V. 1991, ApJ, 378, 656

________ 1992, ApJ, 393, 697

________ 1993, ApJ, 418, 187

Nowak, M. A., Wagoner, R. V., Begelman, M. C., & Lehr, D. E. 1997, ApJ, 477, L91

Oke, J. B. 1967, ApJ, 150, L5

Penston, M. V., & Cannon, R. D. 1970, Roy. Obs. Bull., No. 159

Perez, C. A., Silbergleit, A. S., Wagoner, R. V., & Lehr, D. E. 1997, ApJ, 476, 589

Pesce, J. E., et al. 2001, ApJ, 556, L79

Shimshoni, M. 1971, Geophys. JRAS, 23, 373

Staubert, R., Konig, M., Friedrich, S., Lamer, G. Sood, R. K., Jamers, S. D., & Sharma, D. P. 1994, A&A, 288, 513

Stockton, A., & MacKenty, J. W. 1983, Nature, 305, 678

Sulentic, J. W., & Arp, H. A. 1987, ApJ, 319, 687

Sunyaev, R. A. 1973, Sov. Astron., 16, 941

Taylor, M., Nelson, M. J., Bless, R. C., Dolan, J. F., Elliot, J. L., Percival, J. W., Robinson, E. L., & van Citters, G. W. 1993, ApJ, 413, L125

Ulrich, M-H., Maraschi, L., & Urry, C. M. 1997, ARA&A, 35, 445

Wagner, S. J., & Witzel, A. 1995, ARA&A, 33, 163

Webb, W., & Malkan, M. 2000, ApJ, 540, 652

Welsh, W. F., Peterson, B. M., Koratkar, A. P., & Korista, K. T. 1998, ApJ, 509, 118

Winkler, H., et al. 1992, MNRAS, 257, 659

FIGURE CAPTIONS

Fig. 1. The counting rate from 3C249.1 during the first observation in Table 1. One second sample times were used in the F140LP filter (1400 - 3000 Å).

Fig. 2. The PSF of the data set in Fig. 1. The ordinate is the Fisher g statistic (Simshoni 1971) at the frequency in cycles per 2688 s.

Fig. 3. The ACF of the data set in Fig. 1 for lag times from 1 s to 1344 s.

Fig. 4. The counting rate from NGC 6814 during our three observations. The gaps are caused by Earth occultations.

Fig. 5. The counting rate during the first 200 s of the first observation of 3C371 at 1 s sample time. The distribution of intervals between photon arrival times is consistent with Poisson statistics.

Fig. 6. The first 3C371 data set rebinned into 45 s long samples after correction for the breathing effect. The exposure time is still continuous. The ordinate is the counting rate in counts per 45 s. The error bars are $\pm 1\sigma$ in length.

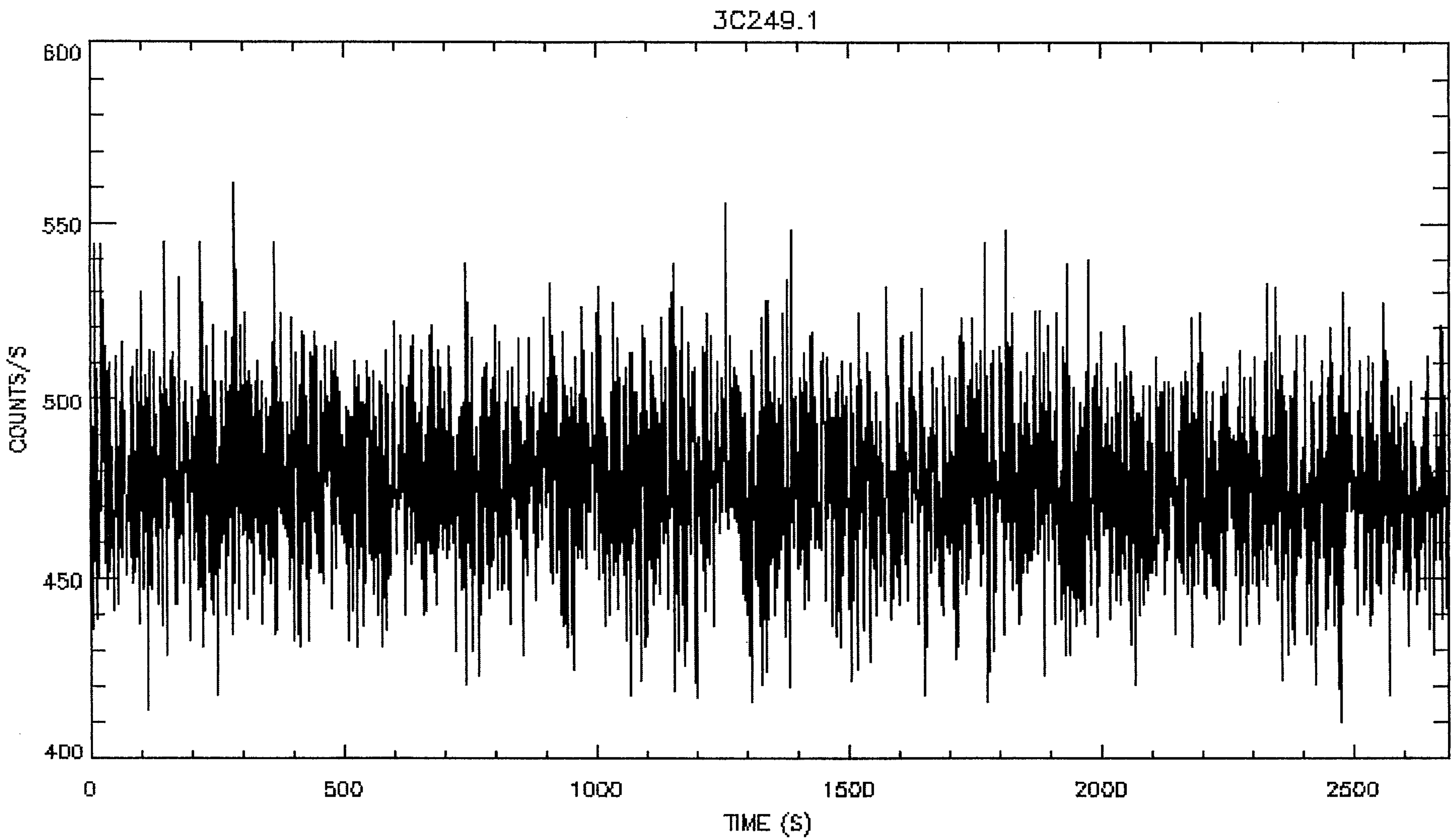
3C249.1
600
550
500
450
400
COUNTS/S
0
500
1000
1500
2000
2500
TIME (S)

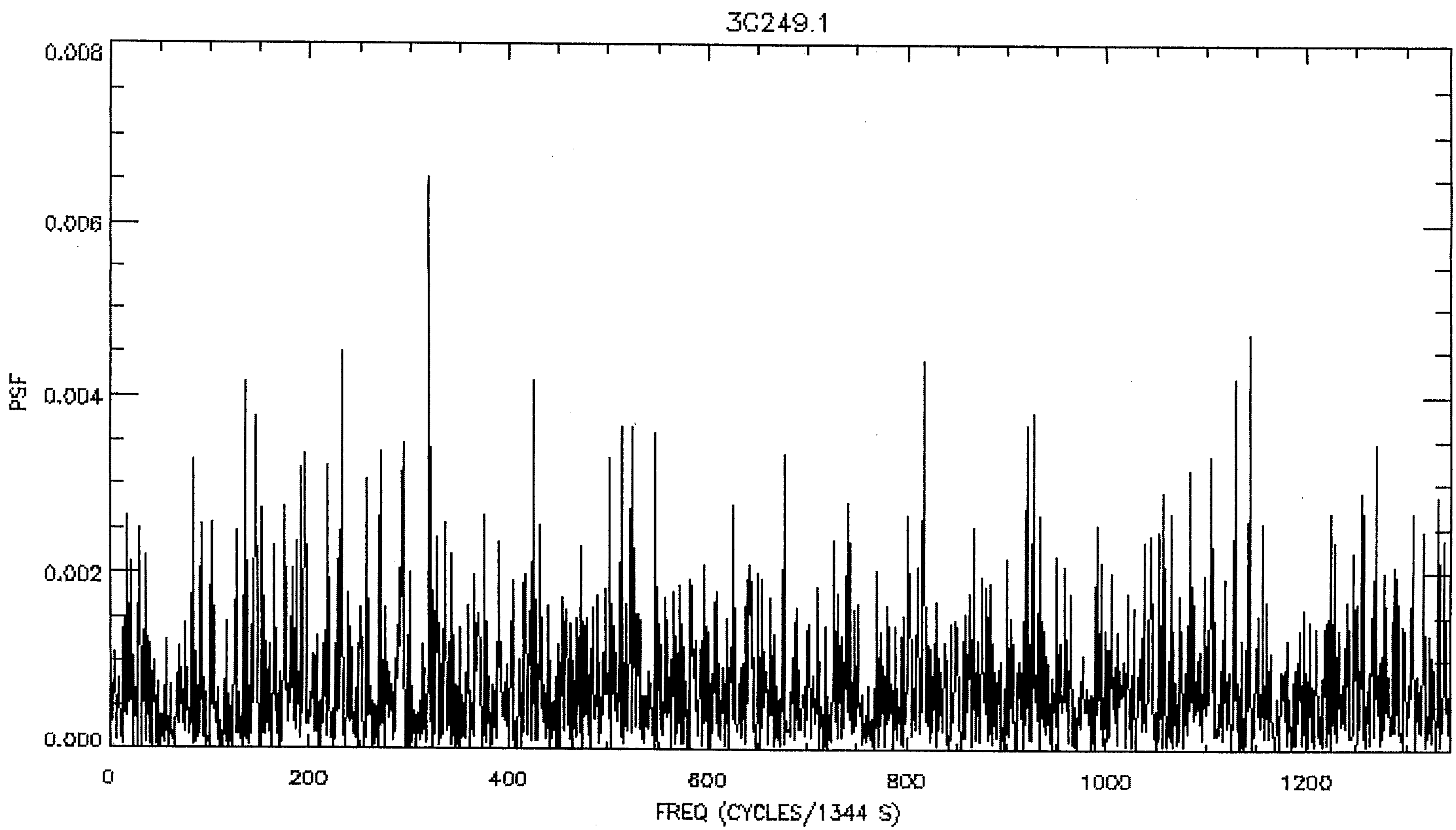
3C249.1
0.008
0.006
0.004
0.002
0.000
PSF
0
200
400
600
800
1000
1200
FREQ (CYCLES/1344 S)

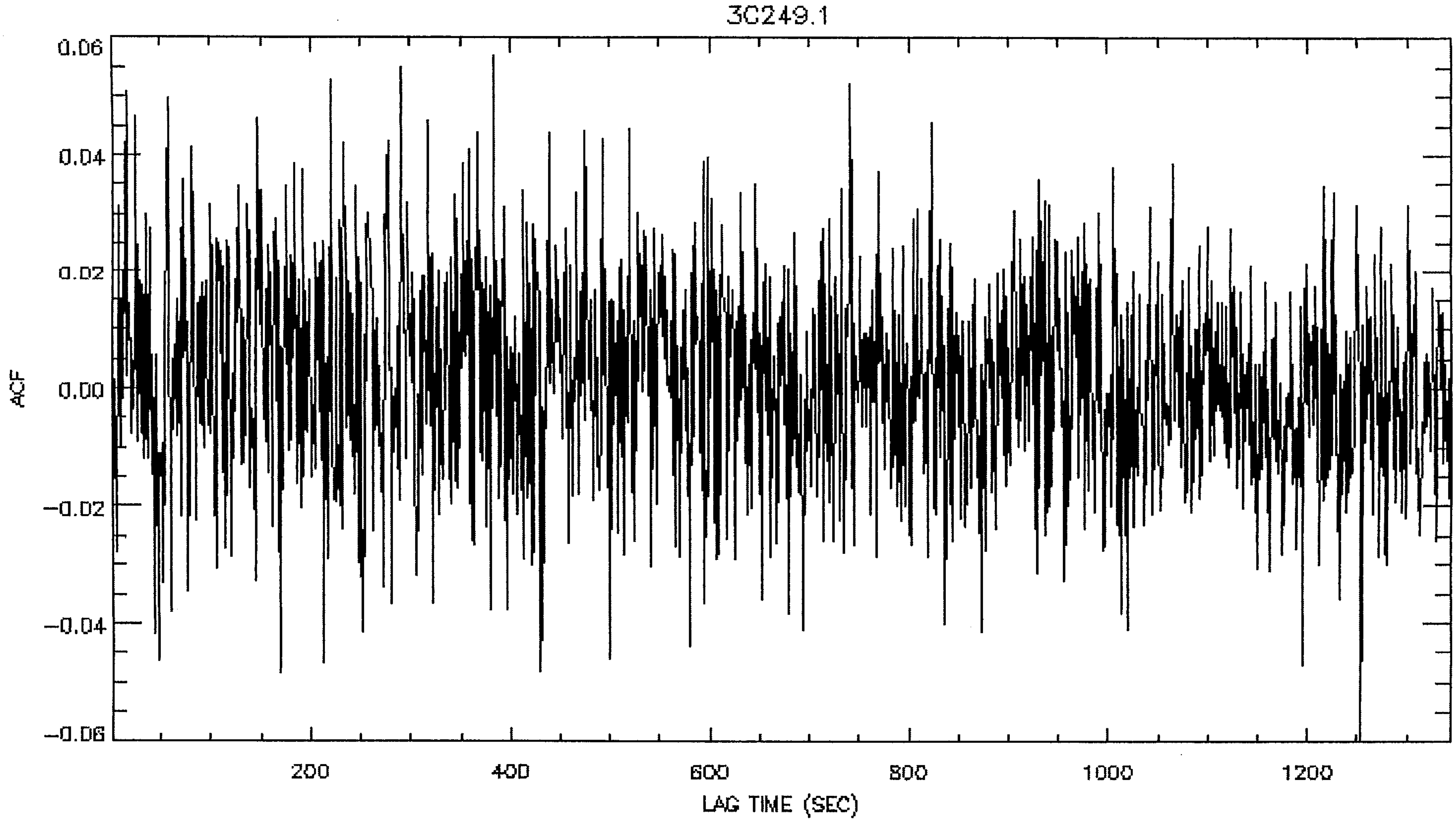

3C249.1
0.06
0.04
0.02
0.00
−0.02
−0.04
−0.06
ACF
200
400
600
800
1000
1200
LAG TIME (SEC)

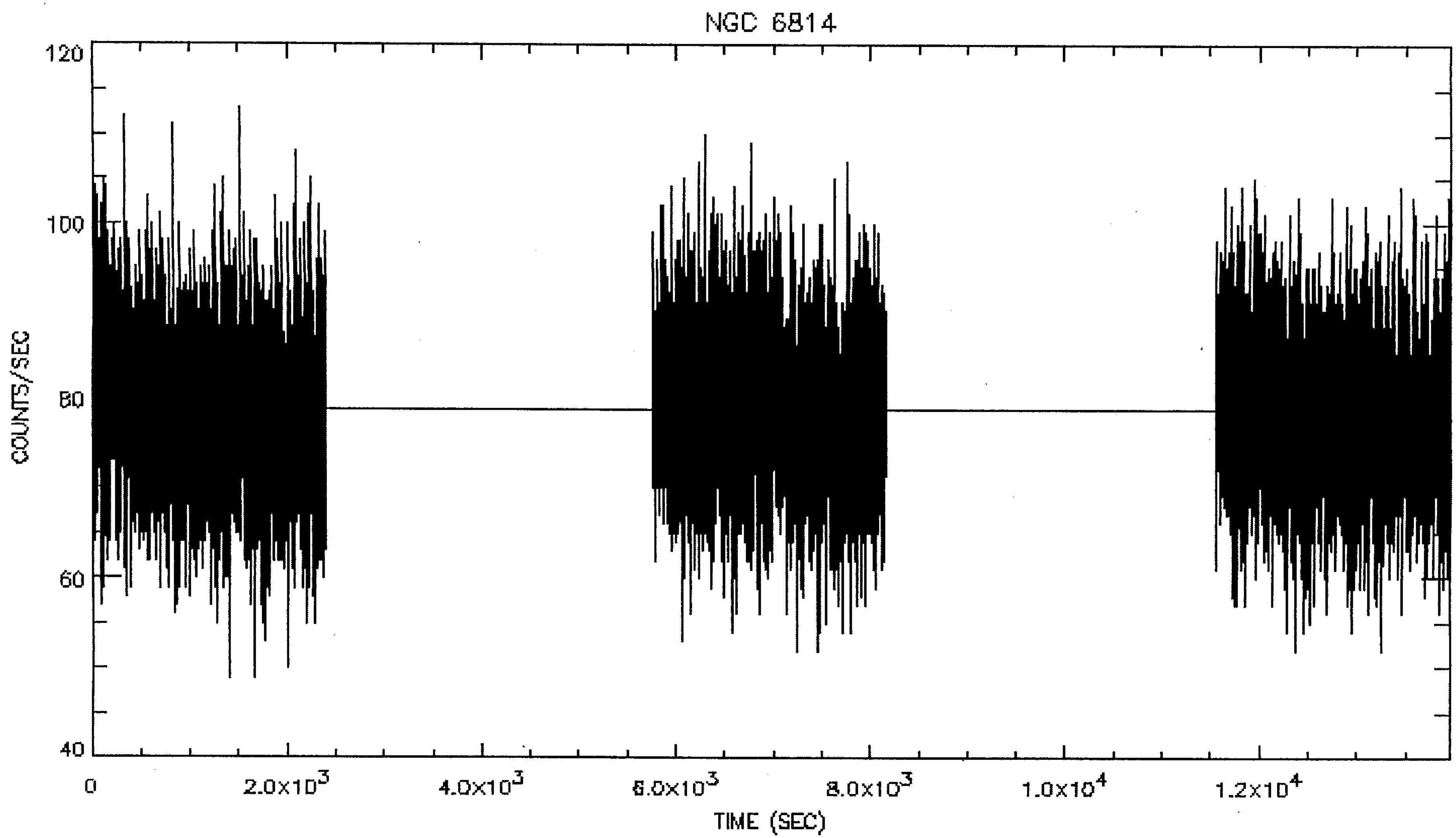
NGC 6814
COUNTS/SEC
120
100
80
60
40
0
2.0x10^3
4.0x10^3
6.0x10^3
8.0x10^3
1.0x10^4
1.2x10^4
TIME (SEC)

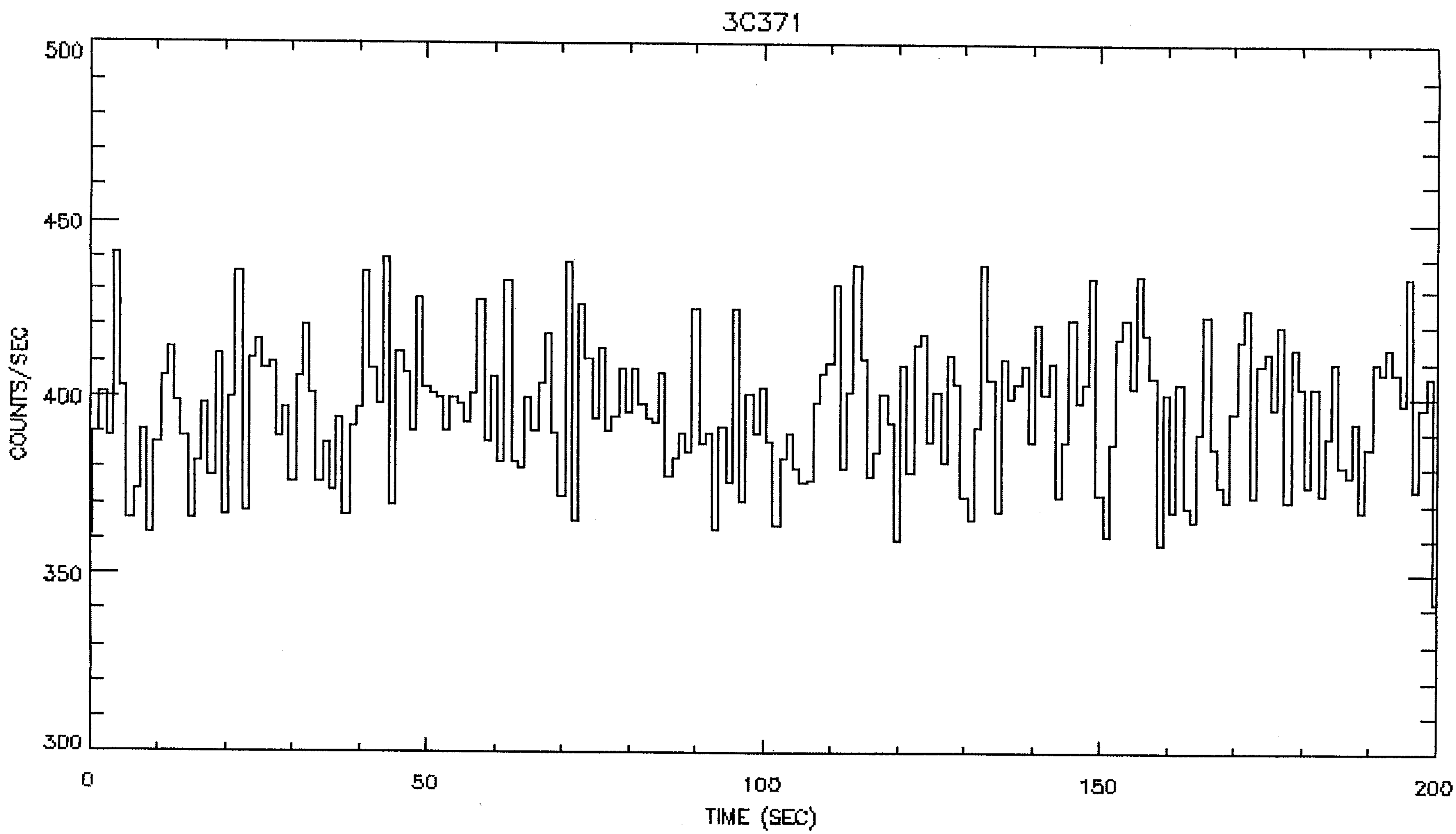
3C371
COUNTS/SEC
500
450
400
350
300
0
50
100
150
200
TIME (SEC)

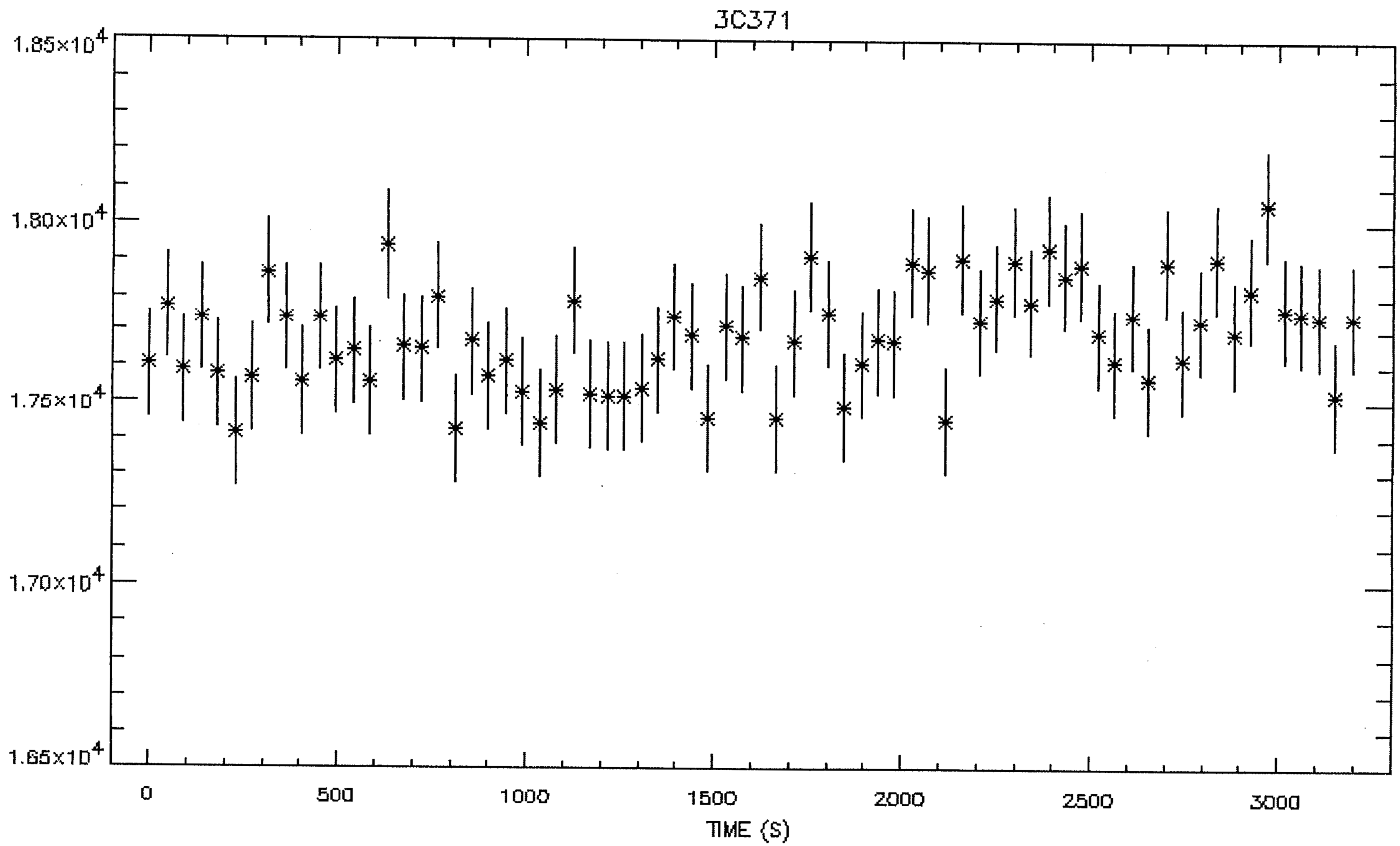
3C371
1.85×10^4
1.80×10^4
1.75×10^4
1.70×10^4
1.65×10^4
0
500
1000
1500
2000
2500
3000
TIME (S)